MJFAS MALAYSIAN JOURNAL OF FUNDAMENTAL AND APPLIED SCIENCES
PRINT ISSN: 2289-5981 | ONLINE ISSN: 2289-599X

RESEARCH ARTICLE

Adsorption isotherms and kinetics of phosphate on waste mussel shell

Nur Atikah Abdul Salim [a, b], Mohd Hafiz Puteh [a, b, *], Abdull Rahim Mohd Yusoff [c, *], Noorul Hudai Abdullah [d], Mohamad Ali Fulazzaky [e], Mohd A'ben Zulkarnain Rudie Arman [a], Mohd Hairul Khamidun [f], Muhammad Abbas Ahmad Zaini [g], Achmad Syafiuddin [a], Noraziah Ahmad [a], Zainab Mat Lazim [a], Maria Nuid [a], Nur Azmira Zainuddin [a]

[a] *School of Civil Engineering, Faculty of Engineering, Universiti Teknologi Malaysia, 81310 UTM Johor Bahru, Johor, Malaysia*
[b] *Centre for Environmental Sustainability and Water Security, Universiti Teknologi Malaysia, 81310 Skudai, Johor, Malaysia*
[c] *Faculty of Science, Universiti Teknologi Malaysia, 81310 UTM Johor Bahru, Johor, Malaysia*
[d] *Centre for Diploma Studies, Faculty of Civil Engineering, Universiti Tun Hussein Onn Malaysia, 84600 Muar, Johor, Malaysia*
[e] *Department of Postgraduate Studies, Djuanda University, 16720 Bogor, Indonesia*
[f] *Faculty of Civil and Environmental Engineering, Universiti Tun Hussein Onn Malaysia, 86400 UTHM Batu Pahat, Johor, Malaysia*
[g] *School of Chemical and Energy Engineering, Faculty of Engineering, Universiti Teknologi Malaysia, 81310 UTM Johor Bahru, Johor, Malaysia*

* *Corresponding author: mhafizputeh@utm.my; rahim@kimia.fs.utm.my*

Article history
Received 6 January 2020
Revised 13 February2020
Accepted 19 March 2020
Published Online 15 June 2020

Graphical abstract

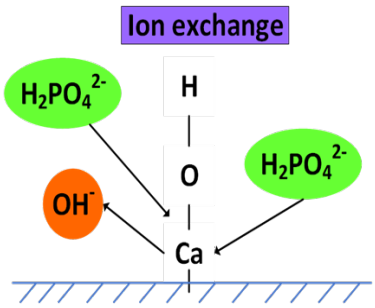

Abstract

In this study, removal of phosphate (PO_4^{3-}) from aqueous solutions using waste mussel shell (WMS) was examined. The physicochemical characteristics of WMS were identified. In the batch experiments, the effects of contact time and adsorbent dosage (*m*) on the PO_4^{3-} adsorption by the WMS were scrutinised. The maximum PO_4^{3-} removal efficiency (*E*) was 83.4% at 144 h contact time for WMS dosage of 10 g. A comparison of kinetic models applied to the adsorption of PO_4^{3-} onto WMS was evaluated using pseudo-first-order (PFO) and pseudo-second-order (PSO) kinetic models. The experimental data was fitted well with the PSO kinetic model. In the isotherm studies, Langmuir and Freundlich isotherm models were applied. The Langmuir isotherm model was well described with the PO_4^{3-} adsorption. The results indicated that WMS has a good potential to adsorb PO_4^{3-} from water and thus could improve environmental quality. Furthermore, this study investigated on how the Langmuir isotherm for basic adsorption could be applied to predict *E* or required *m* under a given set of initial conditions (i.e., initial solute concentration, solution volume, and adsorbent dosage). This was accomplished by combining the Langmuir isotherm with mass balance of solutes between liquid solution and solid adsorbent phases.

Keywords: Adsorption, phosphate, waste mussel shell, Langmuir isotherm model, pollution removal efficiency

INTRODUCTION

Phosphorus (P) is an important element to all living organisms. However, high concentration of P released into natural water strongly accelerates eutrophication (Mezenner & Bensmaili, 2009). Eutrophication is the aging process for water bodies, which causes algal blooms, aquatic life death, and decrement in water quality (Song et al., 2011). The principal forms of P in water are orthophosphate, polyphosphate, and organically bound phosphate (Caravelli et al., 2010). The most common P compound in wastewater is orthophosphate (Hussain et al., 2011). The effects of the discharge of P to receiving water has led to legislations such as those by the European Union (EU) and United State Environmental Protection Agency (USEPA). The EU permits the effluent limit of total phosphorus (TP) ranging from 1 to 2 $mg \cdot L^{-1}$ for 10,000–100,000 population equivalent. Meanwhile, the USEPA follows a TP limit of 0.5–0.8 $mg \cdot L^{-1}$ to control eutrophication (Abdul Salim et al., 2018).

Many water treatment methods are used to remove P from water, such as biological phosphorus removal, chemical precipitation, and adsorption. The biological process to treat wastewater can be highly variable due to operational difficulties (Oladoja et al., 2012). Furthermore, the chemical treatment entails high chemical costs and increased sludge amount (Fulazzaky et al., 2015). Among these treatment methods, the adsorption process is superior to other methods. This technique has a simple operation and produces small volume of sludge. Nowadays, considerable attention has been paid on economical and environmental concerns to the study of using different types of low-cost adsorbents such as rice straw (Luo et al., 2019), oyster shell (Nam et al., 2017), eggshell (Torit & Phihusut, 2018), and cockle shell (Kim et al., 2018).

In this study, the selection of mussel shell as a low-cost alternative adsorbent for PO_4^{3-} removal was favourable due to its high availability in Malaysia. WMS contains calcium carbonate, which enables it to adsorb PO_4^{3-} from water (Kim et al., 2018). The objectives of this work were to determine the adsorption kinetic and isotherm for the adsorption of PO_4^{3-} onto WMS based on the data of batch experiments and to elucidate how basic adsorption isotherm (i.e., Langmuir isotherm model) combined with simple mass/material balance could be applied to estimate removal efficiency or required adsorbent amount according to a given set of initial conditions.

ADSORPTION KINETICS AND ISOTHERMS

Kinetic adsorption models

The adsorption kinetic is of interest for many aspects of surface chemistry, from understanding adsorption/desorption mechanisms to more practical problems such as purification of water (Abdul Salim et al., 2018; Singh et al., 2018), food processing (Zhong et al., 2019), flue gas separation (Wang et al., 2018) and catalysis (Dzade & De Leeuw, 2018).

Pseudo-first-order model

The first-order rate equation is commonly expressed as (Ho & McKay, 2000):

$$\ln(q_e - q_t) = \ln(q_e) - k_1 t_i \quad (1)$$

where q_e is the equilibrium amount of PO_4^{3-} adsorbed (mg·g^{-1}), q_t is the amount of PO_4^{3-} adsorbed at adsorption time (mg·g^{-1}), k_1 is a rate constant of PFO equation (min^{-1}) and t_i is the adsorption time (min).

The values of k_1 and ln q_e can be evaluated from the slope and intercept of plot ln($q_e - q_t$) versus t_i, respectively (Table 1). When the curve of plotting ln($q_e - q_t$) versus t_i shows a straight line, the adsorption kinetic follows a PFO model.

Pseudo-second-order model

The second-order rate equation can be expressed in the linear form of (Ho, 2006):

$$\frac{t_i}{q_t} = \frac{1}{k_2 q_e^2} + \frac{t_i}{q_e} \quad (2)$$

where q_t (mg·g^{-1}) is the amount of PO_4^{3-} adsorbed at adsorption time, q_e is the amount of PO_4^{3-} adsorbed at equilibrium time (mg·g^{-1}), k_2 is a rate constant of PSO model (min^{-1}) and t_i is the adsorption time (min).

The adsorption kinetic obeys a PSO model when the plot of t_i/q_t versus t_i gives a straight line (Köse & Kivanç, 2011). The values of k_2 and q_e can be evaluated from the intercept and slope of plot t_i/q_t versus t_i, respectively (Table 1). The PFO and PSO models have been successfully applied for the adsorption of PO_4^{3-} from aqueous solution (Abdul Salim et al., 2018; Chen et al., 2013; Chen et al., 2012; Köse & Kivanç, 2011; Mezenner & Bensmaili, 2009; Oladoja et al., 2012).

Table 1 List of adsorption kinetics models.

Kinetic models	Linear form	Plot	Parameters
PFO	$\ln(q_e - q_t) = \ln(q_e) - k_1 t_i$	ln(q_e – q_t) vs. t_i	q_e (mg·g^{-1}) k_1 (min^{-1})
PSO	$\frac{t_i}{q_t} = \frac{1}{k_2 q_e^2} + \frac{t_i}{q_e}$	$\frac{t_i}{q_t}$ vs. t_i	q_e (mg·g^{-1}) k_2 (min^{-1})

Isotherm adsorption models

The Freundlich and Langmuir equations are commonly used to describe adsorption isotherms. The Freundlich model describes that a heterogeneous surface of adsorbates forms on the surface of adsorbent with multilayer sorption of different energies of adsorption (Boopathy et al., 2013). The Langmuir model assumes that the adsorbent is being saturated when the monolayer adsorbate coverage of adsorbent has attached with a homogenous surface without interactions between the adsorbed molecules (Song et al., 2011).

Freundlich model

The linear form of the Freundlich isotherm can be written as:

$$\ln q_e = \ln K_F + \frac{1}{n} \ln C_e \quad (3)$$

where K_F is the Freundlich constant (mg·g^{-1}), n (dimensionless) is the heterogeneity factor which has a lower value for more heterogeneous surfaces, and C_e is the concentration of the adsorbate in the equilibrium solution (mg·L^{-1}).

The Freundlich isotherm suggests that a plot of ln q_e versus ln C_e should give a straight line intercept at K_F with $1/n$ as slope (Table 2). The adsorption coefficient K_F indicates the affinity of adsorbate–adsorbent. The exponent n is related to energetic heterogeneity of the adsorbent surface and determines either the favourable or unfavourable curve (Zhu et al., 2011).

Langmuir model

The linear form of the Langmuir isotherm can be written as (Yakout & Elsherif, 2010):

$$\frac{1}{q_e} = \frac{1}{K_L q_{max} C_e} + \frac{1}{q_{max}} \quad (4)$$

where q_{max} is the maximum adsorption capacity of the adsorbent (mg·g^{-1}) and K_L is the Langmuir constant (L·mg^{-1}).

The Langmuir isotherm suggests that a plot of $1/q_e$ against $1/C_e$ of the Eq. (4) should give a straight line with $1/K_L q_{max}$ as slope and $1/q_{max}$ intercept at the vertical axis (Table 2). The adsorption coefficient K_L implies the adsorption energy of adsorbate–adsorbent and q_{max} is the maximum adsorption capacity of the adsorbent (Zhu et al., 2011).

Table 2 List of adsorption isotherm models.

Isotherm models	Linear form	Plot	Parameters
Freundlich	$\ln q_e = \ln K_F + \frac{1}{n} \ln C_e$	ln q_e vs. ln C_e	K_F (mg·g^{-1}) n (dimensionless)
Langmuir	$\frac{1}{q_e} = \frac{1}{K_L q_{max} C_e} + \frac{1}{q_{max}}$	$\frac{1}{q_e}$ vs. $\frac{1}{C_e}$	q_{max} (mg·g^{-1}) K_L (L·mg^{-1})

Langmuir isotherm model development

The Langmuir isotherm can be expressed by the following equation (Ho, 2006):

$$q_e = \left(\frac{K_L \cdot C_e}{1 + K_L \cdot C_e}\right) \cdot q_{max} \quad (5)$$

The linear form of the Langmuir isotherm can be written as (Ho, 2006):

$$\frac{1}{q_e} = \left(\frac{1}{K_L \cdot q_{max}}\right) \cdot \frac{1}{C_e} + \frac{1}{q_{max}} \quad (6)$$

In any adsorption experiments, C_e can be measured and q_e can be calculated for a series of different conditions. Then, $1/q_e$ can be plotted as a function of $1/C_e$. When the curve of plotting $1/q_e$ against $1/C_e$ gives a straight line, the adsorption process is satisfied to follow the Langmuir adsorption isotherm. Consequently, two parameters (K_L and q_{max}) can be obtained by using the slope and the intercept to scrutinise the adsorption process.

The q_e in Eq. (5) can also be expressed in terms of solution volume (V) and adsorbent mass (m) as follows (Chung et al., 2015):

$$q_e = \left(\frac{V \cdot C_e^S}{m}\right) \quad (7)$$

The isotherm equation is combined with a mass/material balance (Chung et al., 2015). In a batch studies, the mass balance expression should be obeyed by the following expression:

$$C_i = C_e + C_e^S \quad (8)$$

where C_i is the initial solute concentration in the solution and C_e^S is the concentration of solute adsorbed onto the adsorbent at equilibrium. The q_e in Eq. (5) can be written by the following equation (Chung et al., 2015):

$$q_e = \left(\frac{V \cdot C_e^S}{m}\right) = \frac{V(C_i - C_e)}{m} \quad (9)$$

Substituting Eq. (9) into Eq. (5) gives the second order function, in which C_e is one argument variable as follows (Chung et al., 2015):

$$K_L \cdot C_e^2 + \left(1 + \frac{K_L \cdot q_{max} \cdot m}{V} - K_L \cdot C_i\right) \cdot C_e - C_i = 0 \quad (10)$$

The following expression is in the form of quadratic equation whereby all variables are treated as constants except for C_e. Therefore, by applying the quadratic formula, the value of C_e can be identified as follows (Chung et al., 2015):

$$C_e = \frac{-\left(1 + \left(K_L \cdot q_{max} \cdot \frac{m}{V}\right) - K_L \cdot C_i\right) + \sqrt{\left(1 + \left(K_L \cdot q_{max} \cdot \frac{m}{V}\right) - K_L \cdot C_i\right)^2 + 4K_L \cdot C_i}}{2K_L} \quad (11)$$

The resulting C_e is a function of C_i and m for a specific V with parameters K_L and q_{max}. Therefore, when K_L and q_{max} are gained through the batch adsorption experiments, C_e can be estimated for the given C_i and m in a fixed volume. Furthermore, the removal efficiency (E) can be expressed as:

$$E = \frac{C_i - C_e}{C_i} \quad (12)$$

and thus, E is also a function of C_i and m for a specific V.

For the given C_i and target E, the model equation to estimate the value of m can be gained. The value of m can be obtained by substituting Eq. (9) and Eq. (12) into Eq. (5) to give:

$$m = \frac{V \cdot E}{K_L \cdot q_{max} \cdot (1 - E)} + \frac{V \cdot E}{q_{max}} \cdot C_i \quad (13)$$

Eq. (13) is an explicit equation, whereby m is a function of C_i and E for a specific V with parameters K_L and q_{max}, and thus, the required m can be estimated under a set of C_i and a desired E (Fig. 1).

Therefore, when $m_{Predicted}$ and $E_{Predicted}$ are obtained, adsorption capacity ($q_{Predicted}$) can be estimated by substituting Eq. (12) into Eq. (9), giving:

$$q = \frac{E \cdot C_i \cdot V}{m} \quad (14)$$

Langmuir isotherm parameter evaluation and model calculation

The Langmuir isotherm was fitted to experimental data for PO_4^{3-} with Eq. (6) to evaluate isotherm parameters. The application tool for user form was created using Excel, which allowed input of the Langmuir isotherm parameters and the set of initial experimental conditions. When the parameters and the set of initial experimental conditions were filled in, the removal efficiency and/or the required adsorbent mass for a target efficiency were calculated by the system.

EXPERIMENTAL

Materials

WMS was collected from Pasir Gudang, Johor. The WMS was rinsed with deionized water and then dried in an oven at a temperature of around 28-30 °C for 48 h. The dried WMS was ground by a grinder (Panasonic, Model MX-AC400W, Malaysia) and sieved at 1.18 mm. The dried adsorbent was used for the adsorption of PO_4^{3-} from aqueous solution.

Synthetic solution

The PO_4^{3-} stock solution (i.e., 100 mg·L^{-1}) was prepared by dissolving 0.1433g of analytical grade potassium dihydrogen phosphate (KH_2PO_4) in 1 L deionised water. (Zapater-Pereyra et al., 2014). The synthetic solution was diluted with deionised water to attain the desired concentration. The pH of the synthetic solutions was set at 7.0 for all the batch experiments.

Analytical methods and characterization techniques

The analysis of PO_4^{3-} was performed using HACH DR 6000 UV–Vis Spectrophotometer in accordance with the Standard Methods for the Examination of Water and Wastewater (APHA, 2005) based on the amino acid method. The measurements of pH were made using a portable pH meter (Jenway Model 350 pH meter).

In this work, the adsorbent was previously sputter-coated with gold (Sputter Coater, Bio-Rad Instruments, USA) for surface morphology analysis of the unmodified adsorbents using a scanning electron microscope (SEM, Hitachi, Model TM3000, Japan). The EDX instrument was used to identify the chemical composition of WMS (Energy-Dispersive X-Ray Spectroscopy, Bruker, Model X Flash 6I10, German). An in-depth analysis for the crystal phase composition of adsorbent was carried out using XRD (High Resolution X-Ray Diffractometer, Bruker D8 Advance, Jerman).

Batch experiments

Batch experiments were conducted to determine adsorption isotherm and kinetics. The experiments of kinetic adsorption were conducted by adding 2, 6, and 10 g of the adsorbents into an Erlenmeyer flask containing 100 mL of PO_4^{3-} 5 mg·L^{-1} and shaken at 140 rpm. The concentrations of PO_4^{3-} in each sample solution were monitored at appropriate time intervals until the adsorbent was saturated. The residual concentrations of PO_4^{3-} presented in each Erlenmeyer flask were determined using HACH DR 6000 UV–Vis Spectrophotometer. The PFO and PSO models were used to study the kinetics of the adsorption of PO_4^{3-} onto the adsorbent.

The isotherm experiments were carried out by adding 2, 4, 6, 8, and 10 g of the adsorbent into different Erlenmeyer flasks containing 100 mL of synthetic solution. Each solution was shaken for 1 to 6 days, depending on time period of the isotherm equilibrium of PO_4^{3-}. Sample solution was monitored at appropriate time intervals and then centrifuged at 6000 rpm for 10 min (Hettich, EBA 21, German). The supernatant of PO_4^{3-} concentration was determined using HACH DR 6000 UV–Vis Spectrophotometer. The Freundlich and Langmuir isotherm models were used to study the adsorption isotherm of PO_4^{3-}.

Each batch adsorption experiment was conducted twice. The adsorption capacity (q) and the removal efficiency (E) were calculated by using Eq. (15) and Eq. (16), respectively.

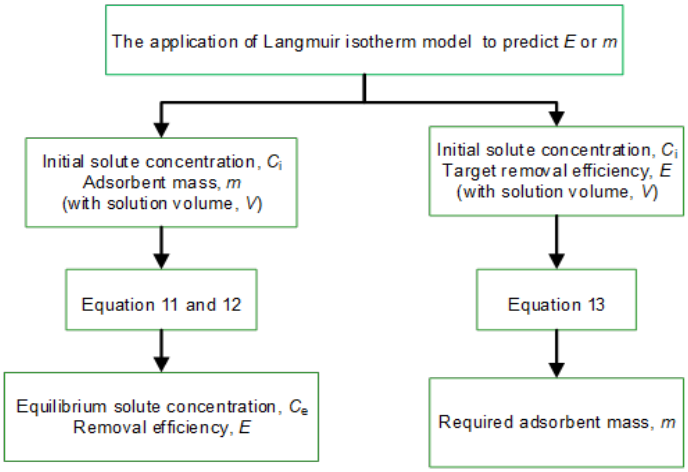

Fig. 1 Diagram for the application of Langmuir isotherm model for the estimation of removal efficiency and adsorbent mass.

$$q = \frac{(C_i - C_f) \times V}{m} \quad (15)$$

$$E = \frac{C_i - C_f}{C_i} \times 100\% \quad (16)$$

where q is the adsorption capacity (mg·g^{-1}), C_i is the initial PO_4^{3-} concentration (mg·L^{-1}), C_f is the PO_4^{3-} concentration in the solution (mg·L^{-1}), m is the mass of adsorbent (g), V is the volume of solution (L) and E is the removal efficiency (%)

RESULTS AND DISCUSSION

Physical and chemical characteristics of the WMS

Table 3 presents the elemental compositions of two natural WMS i.e., WMS from Pasir Gudang and WMS of Abonomar S.L., Spain. The major elemental composition of WMS was Ca and the minor compositions were Na, Fe, and Al, which were higher than those in WMS from Abonomar S.L. (Paradelo et al., 2016). This implied that WMS was mainly comprised of Ca and could be a potentially suitable material for PO_4^{3-} removal from aqueous solution (Kim et al., 2018).

Table 3 Elemental composition of the WMS.

WMS of:	Element composition			
	Ca (%)	Na (%)	Fe (%)	Al (%)
Pasir Gudang[a]	41.69	0.92	0.02	0.02
Abonomar S.L.[b]	28.00	0.52	ND	ND

(1) [a]WMS of Pasir Gudang found in Johor, Malaysia, is the adsorbent used in this study; (2) [b]WMS of Abonomar S.L. found in Pontevedra, Spain, is the WMS in the literature; (3) ND: not detected.

The SEM images were taken to examine the surface morphology of the WMS, as shown in Fig. 2. Fig. 2a (1004× magnification) shows that the WMS has a rough surface. The SEM micrograph image with 2003× magnification (Fig. 2b) exhibits a rough surface with some voids of different sizes presented on the surface of WMS, implying that the availability of high surface area could exhibit higher capability to adsorb PO_4^{3-} from synthetic solution.

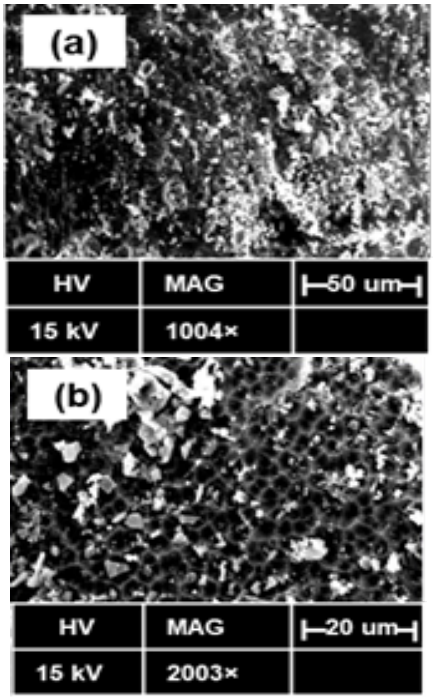

Fig. 2 SEM photomicrograph of WMS: (a) 1004× magnification, (b) 2003× magnification.

The XRD spectra of the WMS sample indicated that aragonite ($CaCO_3$) was the major component while sodium oxide (NaO) was the minor component of the WMS from Pasir Gudang (Fig. 3) and could have more favourable to chemically attract PO_4^{3-} from aqueous solution (Panagiotou et al., 2018). Several researchers have noted that aragonite has good adsorption ability for PO_4^{3-} ions (Vieira et al., 2019).

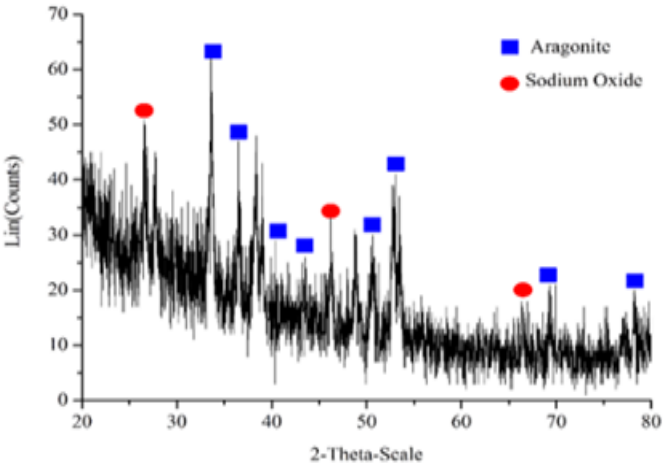

Fig. 3 X-ray diffraction spectra of WMS.

Adsorption of PO_4^{3-} from a synthetic solution onto the WMS

Fig. 4. illustrates the relationship of WMS dosage (m) on both E and q for PO_4^{3-} adsorption onto WMS. Figs. 4a and b show that when the WMS dosage was increased from 2 to 10 g, E for adsorption of PO_4^{3-} was gradually increased from 43.8% to 83.4% while q was gradually decreased from 0.11 to 0.04 mg·g^{-1}. Higher adsorbent amount used in a batch experiment has resulted in more adsorbent surface area that available to adsorb PO_4^{3-} and thus, the percent removal of PO_4^{3-} was increased (Hussain et al., 2011; Köse & Kivanç, 2011; Xiong et al., 2011). The decreasing amount of q with increasing adsorbent dosage was a result of active sites on the WMS surface that remained unsaturated throughout the adsorption experiment (Aydın & Bulut, 2008). Hence, more adsorbent dosage used would appear to be difficult to attain at a saturation state (Abdul Salim et al., 2018). Besides that, the higher amount of adsorbent might cause particle aggregation and interference or repulsive forces between active binding sites and thus, reducing the interaction of PO_4^{3-} with the adsorbent and decreasing the total surface area of the adsorbent (Abdul Salim et al., 2018; Mezenner & Bensmaili, 2009).

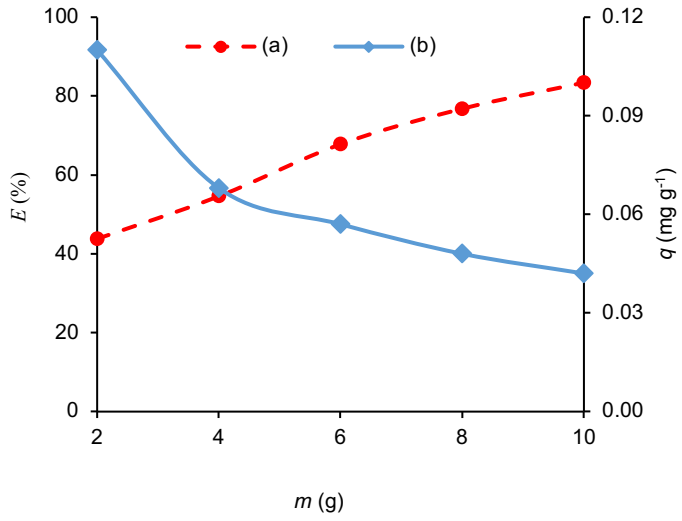

Fig. 4 Relationship between: (a) the removal efficiency and the WMS dosage and (b) the adsorption capacity and the WMS dosage.

Adsorption kinetics of PO_4^{3-} onto the WMS

In this study, the linear plots of PFO (Fig. 5a) and PSO (Fig. 5b) models were used to describe the adsorption kinetics of PO_4^{3-} from synthetic solution (Ho & McKay, 1998). Table 4 shows the kinetic parameters k_1, k_2, and qe for PFO and PSO models.

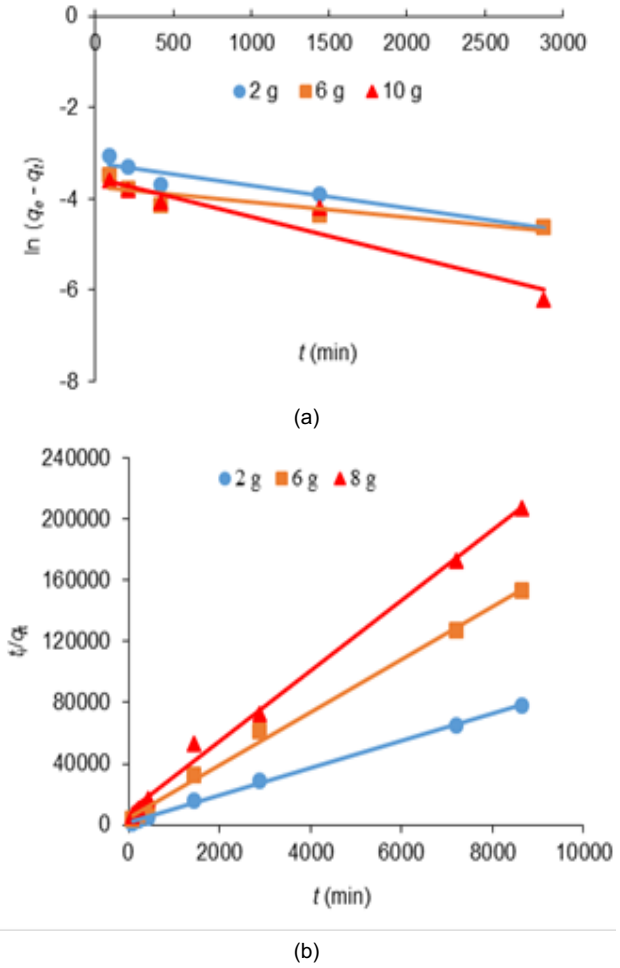

Fig. 5 Linear plots of: (a) PFO model and (b) PSO model for the PO_4^{3-} adsorption onto WMS.

Table 4 Kinetic parameters obtained from the PFO and PSO models for the PO_4^{3-} adsorption onto WMS.

Medium	Amount (g)	Pseudo-first-order model			
		q_e (theo) ($mg \cdot g^{-1}$)	k_1 (min^{-1})	R^2	q_e (exp) ($mg \cdot g^{-1}$)
Synthetic solution	2	0.040	0.0005	0.919	0.110
	6	0.030	0.0004	0.948	0.057
	10	0.036	0.0009	0.959	0.042
Medium	**Amount (g)**	**Pseudo-second-order model**			
		q_e (theo) ($mg \cdot g^{-1}$)	k_2 ($g \cdot mg^{-1} \cdot min^{-1}$)	R^2	q_e (exp) ($mg \cdot g^{-1}$)
Synthetic solution	2	0.112	0.0481	0.999	0.110
	6	0.058	0.0614	0.996	0.057
	12	0.043	0.0643	0.996	0.042

The linear regression analysis of the kinetic models for the adsorption of PO_4^{3-} from a synthetic solution by WMS was shown in Fig. 5. As shown in Table 4, the correlation coefficient for the PSO model ($R^2 > 0.996$) was higher than the for PFO model ($R^2 > 0.919$). This study verified that the PSO model ~~is~~ was more suitable for the adsorption kinetic of PO_4^{3-} from a KH_2PO_4 solution onto WMS compared to the PFO model (Table 4).

According to the results of this study, the adsorption between WMS and PO_4^{3-} could be categorised as chemical adsorption. Chemical adsorption is based on chemical reactions between the adsorbate and the surface sites of the adsorbent (Worch, 2012), in which the adsorption process involves valence forces through sharing or exchanging of electrons between adsorbent and adsorbate through the replacement of OH^- by PO_4^{3-} (Xiong et al., 2017). Similar results have been reported for the adsorption of PO_4^{3-} onto ferric sludge (Song et al., 2011) and methylene blue onto dehydrated peanut hull (Özer et al., 2007), where the value of k_2 increases while the value of q_e decreases with increasing amount of adsorbent.

Adsorption isotherms of PO_4^{3-} onto the WMS

Batch isotherm studies were performed in order to understand the relationship between the amount of the PO_4^{3-} adsorbed per unit mass of WMS and the PO_4^{3-} concentration in the solution at equilibrium. The experimental data for the adsorption of PO_4^{3-} onto WMS was analysed using the linearised forms of the Freundlich (Fig. 6a) and Langmuir (Fig. 6b) models. The Langmuir and Freundlich parameters are listed in Table 5. The correlation coefficient for Langmuir model ($R^2 > 0.882$) was higher than for Freundlich model ($R^2 > 0.877$), indicating that PO_4^{3-} adsorption was more likely a monolayer adsorption process with uniform distribution of energetic adsorption sites on its surface (Lü et al., 2009).

Table 5 The parameters n, K_F, q_{max}, and K_L for the adsorption of PO_4^{3-} onto WMS.

Sample	Freundlich model			Langmuir model		
	n	K_F ($mg \cdot g^{-1}$)	R^2	q_{max} ($mg \cdot g^{-1}$)	K_L ($L \cdot mg^{-1}$)	R^2
Synthetic solution	1.41	0.044	0.877	0.157	0.412	0.882

Application of Langmuir isotherm to estimate adsorbate removal efficiency or required amount of adsorbent

Experimental data of PO_4^{3-} adsorption onto WMS was fitted to the linear forms of Freundlich and Langmuir isotherm models in Eq. (3) and Eq. (4), which are depicted in Fig. 6. The results showed that the Langmuir isotherm model gave a good mathematical model to explain the adsorption equilibrium compared to the Freundlich isotherm model. From the slope and intercept of the plot of $1/q_e$ against $1/C_e$ in Fig. 6(b), the K_L and q_{max} values were attained as listed in Table 5. When the Langmuir isotherm parameters were identified, the removal efficiencies for any set of experimental conditions could be estimated. Eq. (11) was used to get the predicted removal efficiencies as a function of initial concentration of PO_4^{3-} solution for different adsorbent masses of PO_4^{3-} in the range of 2 to 10 g. The predicted data was compared to the experimental data for validation (Table 6a). This finding showed that the Langmuir isotherm model with mass balance was able to predict the removal efficiency by adsorption using initial solute concentration and different adsorbent masses. Furthermore, model verification was conducted to determine the required amount of adsorbent (Table 6b) by using Eq. (13). In addition, when $m_{Predicted}$ and $E_{Predicted}$ were obtained, adsorption capacity ($q_{Predicted}$) could be estimated by using Eq. (14). Fig. 7 shows the practical application of Langmuir isotherm. According to the figure, the removal efficiency could be predicted with different amounts of WMS.

Table 6 Comparison of (a) removal efficiency, E, and (b) required adsorbent mass, m, predicted by Langmuir isotherm with mass balance to experimental data obtained from adsorption of PO_4^{3-} onto WMS.

(a)

Initial conditions		$E_{Experimental}$ (%)	$E_{Predicted}$ (%)	
C_i (mg·L^{-1})	m (g)		Langmuir isotherm	Error (%)
5.0	2.000	43.8	35.8	18.34
5.0	4.000	54.6	58.1	6.50
5.0	6.000	67.8	70.8	4.40
5.0	8.000	76.8	78.1	1.69
5.0	10.000	83.4	82.7	0.89

(b)

Initial conditions		m_E (g)	m_P (g)		q_P (mg·g^{-1})	
C_i (mg·L^{-1})	E_P (%)		Langmuir isotherm	Error (%)	Langmuir isotherm	Error (%)
5.0	38.5	2.000	2.194	9.70	0.088	20.23
5.0	61.0	4.000	4.361	9.02	0.070	2.86
5.0	73.2	6.000	6.554	9.23	0.056	2.03
5.0	80.0	8.000	8.732	9.15	0.046	4.56
5.0	84.1	10.000	10.855	8.55	0.039	7.77

(1) E_P: $E_{Predicted}$; (2) m_E: $m_{Experimental}$; (3) m_P: $m_{Predicted}$; (4) q_P: $q_{Predicted}$

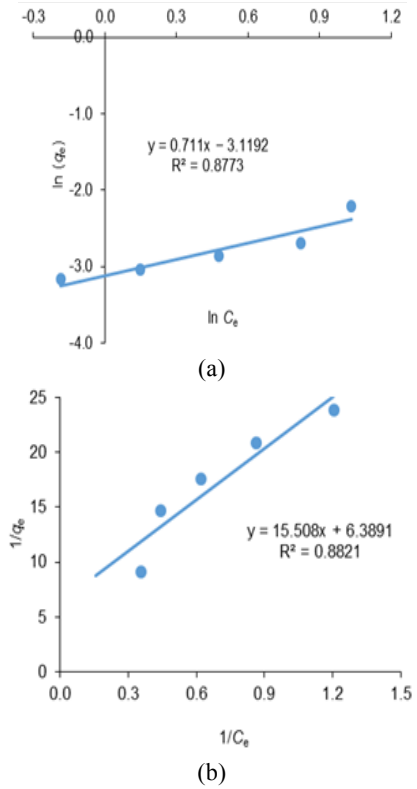

Fig. 6 Linear plots of: (a) Freundlich model and (b) Langmuir model for PO_4^{3-} adsorption.

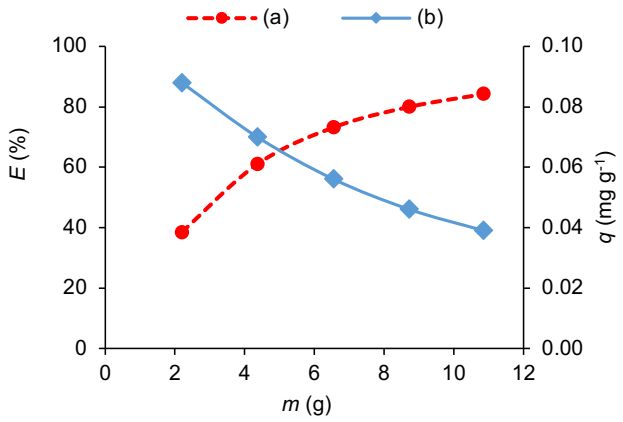

Fig. 7 Relationship of: (dashed line) $E_{Predicted}$ and $m_{Predicted}$ for the adsorption of PO_4^{3-}; (solid line) $q_{Predicted}$ and $m_{Predicted}$ for the adsorption of PO_4^{3-}.

CONCLUSION

In this study, the verification of the isotherm and kinetic models was performed to understand the behaviour of the adsorption of PO_4^{3-} from synthetic solution onto WMS. The adsorption kinetic data was best described by the PSO model, suggesting that chemisorption was involved during the adsorption process. The adsorption of PO_4^{3-} onto WMS was best described by the Langmuir model, suggesting that the adsorption of PO_4^{3-} onto WMS was occurred as monolayer. The result proposed that WMS has a good potential to adsorb PO_4^{3-} from water and thus, improving environmental quality.

ACKNOWLEDGEMENT

The authors would like to acknowledge the Universiti Teknologi Malaysia and the Fundamental Research Grant Scheme provided by the Ministry of Higher Education (NO. 4F956).

REFERENCES

Abdul Salim, N. A., Abdullah, N. H., Khairuddin, M. R., Rudie Arman, M. A. Z., Khamidun, M. H., Fulazzaky, M. A. and Puteh, M. H., (2018). Adsorption of phosphate from aqueous solutions using waste mussel shell. *MATEC Web of Conferences*, 250, 06013.

APHA, AWWA, WEF, *Standard methods for the examination of water and wastewater*, 21st ed. (2005). American Public Health Association, Washington, D.C., 2005.

Aydın, H. and Bulut, Y. (2008). Removal of copper (II) from aqueous solution by adsorption onto low-cost adsorbents. *Journal of Environmental Management*, 87, 37–45.

Boopathy, R., Karthikeyan, S., Mandal, A. B. and Sekaran, G. (2013). Adsorption of ammonium ion by coconut shell-activated carbon from aqueous solution: Kinetic, isotherm, and thermodynamic studies. *Environmental Science and Pollution Research*, 20(1), 533–542.

Caravelli, A. H., Contreras, E. M. and Zaritzky, N. E. (2010). Phosphorous removal in batch systems using ferric chloride in the presence of activated sludges. *Journal of Hazardous Materials*, 177(1–3), 199–208.

Chen, J., Cai, Y., Clark, M. and Yu, Y. (2013). Equilibrium and kinetic studies of phosphate removal from solution onto a hydrothermally modified oyster shell material. *PLoS ONE*, 8(4), 1–10.

Chen, W.-T., Lin, C.-W., Shih, P.-K. and Chang, W.-L. (2012). Adsorption of phosphate into waste oyster shell: thermodynamic parameters and reaction kinetics. *Desalination and Water Treatment*, 47(1–3), 86–95.

Chung, H., Kim, W., Park, J., Cho, J., Jeong, T. and Park, P. (2015). Application of Langmuir and Freundlich isotherms to predict adsorbate removal efficiency or required amount of adsorbent. *Journal of Industrial and Engineering Chemistry*, 28, 241–246.

Dzade, N. Y., and De Leeuw, N. H. (2018). Adsorption and desulfurization mechanism of thiophene on layered fes(001), (011), and (111) surfaces: A dispersion-corrected density functional theory study. *Journal of Physical Chemistry C*, 122(1), 359–370.

El Haddad, M., Regti, A., Laamari, M. R., Slimani, R., Mamouni, R., Antri, S. El. and Lazar, S. (2014). Calcined mussel shells as a new and eco-friendly biosorbent to remove textile dyes from aqueous solutions. *Journal of the Taiwan Institute of Chemical Engineers,* 45(2), 533–540.

Fulazzaky, M. A., Abdullah, N. H., Mohd Yusoff, A. R. and Paul, E. (2015). Conditioning the alternating aerobic-anoxic process to enhance the removal of inorganic nitrogen pollution from a municipal wastewater in France. *Journal of Cleaner Production*, 100(3), 195–201.

Ho, Y.S. (2006). Isotherms for the sorption of lead onto peat: Comparison of linear and non-linear methods. *Polish Journal of Environmental Studies*, 15(1), 81–86.

Ho, Y. S. and McKay, G. (1998). A Comparison of chemisorption kinetic models applied to pollutant removal on various sorbents. *Process Safety and Environmental Protection*, 76(4), 332–340.

Ho, Y. S. and McKay, G. (2000). The kinetics of sorption of divalent metal ions onto sphangnum moss peat. *Water Research*, 34(3), 735–742.

Ho, Y. S. (2006). Review of second-order models for adsorption systems. *Journal of Hazardous Materials*, 136(3), 681–689.

Hussain, S., Aziz, H. A., Isa, M. H., Ahmad, A., Van Leeuwen, J., Zou, L. and Umar, M. (2011). Orthophosphate removal from domestic wastewater using limestone and granular activated carbon. *Desalination*, 271(1–3), 265–272.

Kaya, E. M. Ö., Özcan, A. S., Gök, Ö. and Özcan, A. (2013). Adsorption kinetics and isotherm parameters of naphthalene onto natural and chemically modified bentonite from aqueous solutions. *Adsorption*, 19(2–4), 879–888.

Kim, Y., Kim, D., Kang, S. W., Ham, Y. H., Choi, J. H., Hong, Y. P., and Ryoo, K. S. (2018). Use of powdered cockle shell as a bio-sorbent material for phosphate removal from water. *Bulletin of the Korean Chemical Society*, 39(12), 1362–1367.

Köse, T. E. and Kivanç, B. (2011). Adsorption of phosphate from aqueous solutions using calcined waste eggshell. *Chemical Engineering Journal*, 178, 34–39.

Lü, J., Sun, L., Zhao, X., Lu, B., Li, Y. and Zhang, L. (2009). Removal of phosphate from aqueous solution using iron-oxide-coated sand filter media: Batch studies. *Proceedings-2009 International Conference on Environmental Science and Information Application Technology*, ESIAT 2009, 1, 639–644.

Luo, L., Wang, G., Shi, G., Zhang, M., Zhang, J., He, J., Deng, O. (2019). The characterization of biochars derived from rice straw and swine manure, and their potential and risk in N and P removal from water. *Journal of Environmental Management*, 245, 1–7.

Mezenner, N. Y. and Bensmaili, A. (2009). Kinetics and thermodynamic study of phosphate adsorption on iron hydroxide-eggshell waste. *Chemical Engineering Journal*, 147(2–3), 87–96.

Nam, G., Choi, Y. H., Lee, N., and Ahn, J. W. (2017). Effect by alkaline flocculation of algae and phosphorous from water using a calcined waste oyster shell. *Water (Switzerland)*, 9(9), 1–11.

Oladoja, N. A., Ahmad, A. L., Adesina, O. A. and Adelagun, R. O. A. (2012). Low-cost biogenic waste for phosphate capture from aqueous system. *Chemical Engineering Journal*, 209, 170–179.

Oladoja, N. A., Ololade, I. A., Adesina, A. O., Adelagun, R. O. A. A. and Sani, Y. M. (2013). Appraisal of gastropod shell as calcium ion source for phosphate removal and recovery in calcium phosphate minerals crystallization procedure. *Chemical Engineering Research and Design*, 91(5), 810–818.

Özer, D., Dursun, G. and Özer, A. (2007). Methylene blue adsorption from aqueous solution by dehydrated peanut hull. *Journal of Hazardous Materials*, 144(1–2), 171–179.

Panagiotou, E., Kafa, N., Koutsokeras, L., Kouis, P., Nikolaou, P., Constantinides, G., and Vyrides, I. (2018). Turning calcined waste egg shells and wastewater to Brushite: Phosphorus adsorption from aqua media and anaerobic sludge leach water. *Journal of Cleaner Production*, 178, 419–428.

Paradelo, R., Conde-Cid, M., Cutillas-Barreiro, L., Arias-Estévez, M., Nóvoa-Muñoz, J. C. C., Álvarez-Rodríguez, E. and Núñez-Delgado, A. (2016). Phosphorus removal from wastewater using mussel shell: Investigation on retention mechanisms. *Ecological Engineering*, 97, 558–566.

Song, X., Pan, Y., Wu, Q., Cheng, Z. and Ma, W. (2011). Phosphate removal from aqueous solutions by adsorption using ferric sludge. *Desalination*, 280(1–3), 384–390.

Singh, N. B., Nagpal, G., Agrawal, S., and Rachna. (2018). Water purification by using adsorbents: A review. *Environmental Technology and Innovation*, 11, 187–240.

Torit, J., and Phihusut, D. (2018). Phosphorus removal from wastewater using eggshell ash. *Environmental Science and Pollution Research*, 1-9.

Wang, Y., Du, T., Qiu, Z., Song, Y., Che, S., and Fang, X. (2018). CO_2 adsorption on polyethylenimine-modified ZSM-5 zeolite synthesized from rice husk ash. *Materials Chemistry and Physics*, 207, 105–113.

Vieira, B., Coelho, L. H. G., and De Jesus, T. A. (2019). Phosphate sorption in shellfish shell (Venerupis pulastra) Substrates: Development of green and low-cost technology for tertiary treatment of effluents. *Journal of Environmental Engineering (United States)*, 145(2), 1–11.

Worch, E. (2012). *Adsorption technology in water treatment: fundamentals, processes, and modeling*. (Walter de Gruyter, Germany, 2012).

Xiong, J., Qin, Y., Islam, E., Yue, M. and Wang, W. (2011). Phosphate removal from solution using powdered freshwater mussel shells. *Desalination*, 276(1–3), 317–321.

Xiong, W., Tong, J., Yang, Z., Zeng, G., Zhou, Y., Wang, D. and Cheng, M. (2017). Adsorption of phosphate from aqueous solution using iron-zirconium modified activated carbon nanofiber: Performance and mechanism. *Journal of Colloid and Interface Science*, 493, 17–23.

Yakout, S. M. and Elsherif, E. (2010). Batch kinetics, isotherm and thermodynamic studies of adsorption of strontium from aqueous solutions onto low cost rice-straw based carbons. *Carbon - Science and Technology*, 3(1), 144–153.

Zapater-Pereyra, M., Malloci, E., van Bruggen, J. J. A. and Lens, P. N. L. (2014). Use of marine and engineered materials for the removal of phosphorus from secondary effluent. *Ecological Engineering*, 73, 635–642.

Zhong, W., Li, X., Yang, H., and Li, E. (2019). A novel, effective, and feasible method for deacidifying kiwifruit wine by weakly basic ion exchange resins. *Journal of Food Process Engineering,* 42(2), 1–9.

Zhu, W. L., Cui, L. H., Ouyang, Y., Long, C. F. and Tang, X. D. (2011). Kinetic adsorption of ammonium nitrogen by substrate materials for constructed wetlands. *Pedosphere*, 21(4), 454–463.